Omega-shaped Geometries of Reflectarray Resonant Elements with Low Cross-polarization for Wideband and Dual-Polarization Use

Daichi Higashi*, Hiroyuki Deguchi, and Mikio Tsuji

Abstract—This paper presents low cross-polarization single-layer reflectarray elements for dual-polarization use. These elements have an omega-shaped symmetrical structure to realize the cross-polarization reduction and also provide parallel linear reflection-phase properties with almost the same slop characteristics for the frequency, thereby achieving the desirable reflection phase range more than 360° over the wide frequency range. To verify effectiveness of the proposed elements, a reflectarray antenna with an offset feed is constructed by them, and wideband frequency characteristics are also confirmed at Ku-band numerically and experimentally.

1. INTRODUCTION

A reflectarray are composed of many reflecting elements printed on a conductor-backed dielectric substrate [1]. So, it has a low-profile, thin, and flat structure and also simple feed system, compared with conventional parabolic reflectors. The phase distribution on its aperture is controlled by arranging various resonant elements with different resonant frequency, thereby changing the reflecting direction. In recent years, reflectarrays have been applied to a lot of applications such as deployable reflector antennas [2], millimeter-wave imaging systems [3] and FSR(frequency selective reflector) to eliminate blind area [4]. In general, wideband, dual-polarization and low cross-polarization properties are required for a reflectarray. However, it has a major drawback which is narrow bandwidth operation because the reflection-phase property of each element based on resonance greatly depends on the frequency. To improve the antenna bandwidth in reflectarray, linearization of reflection phase response for the frequency can be realized in some investigation by using thick substrate [5], double square-rings [6], stacked patches [7], multi-resonant elements with low-cross polarization [8], phase-delay lines [9] and so on. We have also reported in [10–14] to improve the bandwidth based on multi-resonant behavior for single- and dual-polarization use. The elements proposed in [14] have broadband property, but cause high-level cross-polarization (more than about −10 dB) over the wide frequency range. Therefore, it is necessary to suppress cross polarization, while keeping wide-band co-polarization properties. Therefore, this paper presents new reflectarray elements to suppress cross polarization [15]. These elements have linear phase lines and the desirable reflection-phase range of 360° for the frequency response. To show effectiveness of the proposed elements, a Ku-band reflectarray antenna is constructed by them and is evaluated by comparison of the radiation patterns between the calculated and the measured results.

2. ANALYTICAL METHOD

Figure 1(a) shows periodic reflectarray elements. Assuming an infinite periodic array, the reflection phase for an incident plane wave can be calculated by the method of moments (MoM) based on the

spectral domain Green's function with periodical boundary condition [16, 17]. Fig. 1(b) shows a unit cell $(d_x \times d_y)$ divided into sub-cells $(\Delta x \times \Delta y)$, and Fig. 1(c) shows the roof-top sub-domain basis function expanding unknown current distributions on the conductor strip element in the x and the y directions. The simultaneous linear equations in the MoM are formulated by using FFT and are solved by the conjugate gradient method (CGM). The scattered electric field from the reflectarray that is derived by enforcing Floquet's periodicity condition can be expressed as follows:

$$\begin{bmatrix} E_x^{(s)}(x,y) \\ E_y^{(s)}(x,y) \end{bmatrix} = \sum_{p=-\infty}^{\infty} \sum_{q=-\infty}^{\infty} \begin{bmatrix} \tilde{G}_{xx} & \tilde{G}_{xy} \\ \tilde{G}_{yx} & \tilde{G}_{yy} \end{bmatrix} \cdot \begin{bmatrix} \tilde{J}_x(k_{xp}, k_{yq}) \\ \tilde{J}_y(k_{xp}, k_{yq}) \end{bmatrix} e^{jk_{xp}x} e^{jk_{yq}y}$$

where $E_x^{(s)}$ and $E_y^{(s)}$ represent the x and the y components of the scattered electric field, respectively. The transformed derivatives, the dyadic spectral Green's function and their constants are incorporated into $\tilde{G}_{xx}$, $\tilde{G}_{xy}$, $\tilde{G}_{yx}$ and $\tilde{G}_{yy}$ to simplify the notation. k_0 is the wave number in the free space, and also k_{xp} and k_{yq} can be expressed as $k_{xp} = k_0 \sin\theta\cos\phi + 2\pi p/d_x$ and $k_{yq} = k_0 \sin\theta\sin\phi + 2\pi q/d_y$, respectively. The indices (p, q) represents Floquet's harmonics. $\tilde{J}_x$ and $\tilde{J}_y$ are the Fourier transforms of the x component J_x and the y component J_y of the unknown currents, respectively. Applying the boundary condition $\mathbf{E}^{(i)} + \mathbf{E}^{(s)} = \mathbf{0}$ on the conductor plates, we can solve unknown currents by using Galerkin's procedure for the currents J_x and J_y expanded in terms of the roof-top basis functions as shown in Fig. 1(c).
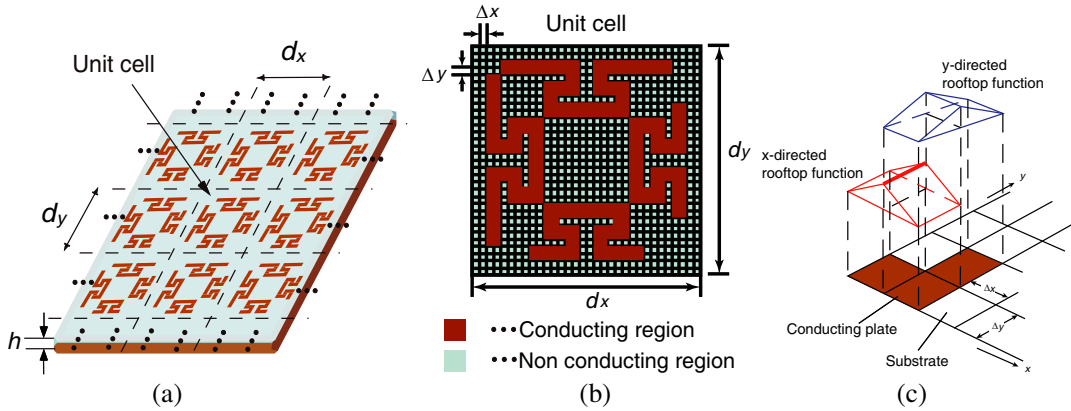
Figure 1. Analysis model for MoM. (a) Periodic reflectarray elements. (b) Unit cell. (c) Roof-top basis function.

3. INVESTIGATION OF REFLECTARRAY ELEMENTS

3.1. Proposed Elements

Figure 2 shows geometries of the element's shape developed by the authors for dual-polarization and wide-band reflectarray [13–15]. To realize the dual-polarization use, the additional two resonant elements are put at the perpendicular as shown in Fig. 2(a). Then, the four resonant elements are modified convexly to achieve wideband property as shown in Fig. 2(b). When longer element's length is needed, the adjacent elements contact with each other. To avoid such a contact, we modified convex part as shown in Fig. 2(c), so that this type of element shape make it possible to extend the wider frequency range. However, these elements generate un-negligible cross-polarized component because of asymmetric element's arrangement. So, it is necessary to lower the height of convex part. As a result, the convex part is modified into an Omega-shape with symmetrical structure as shown in Fig. 2(d). The dimensions at the center frequency 15 GHz are as follows, the periodic of a unit cell $d_x = d_y = 9.6$ [mm], the thickness of supported dielectric substrate $h = 3.0$ [mm] with relative permittivity 1.68 ($\tan\delta = 0.001$), the strip width of the elements $w = 0.6$ [mm], and the degree of convex $B = 1.8$ [mm]. Analytical model to calculate the reflection phase characteristics is shown in Fig. 3, where the incident angle $\theta_s = 30°$. The
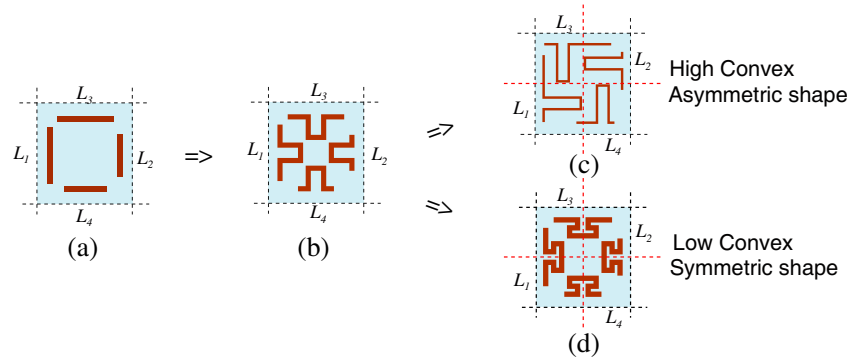
Figure 2. Geometries of the elements as a unit cell.
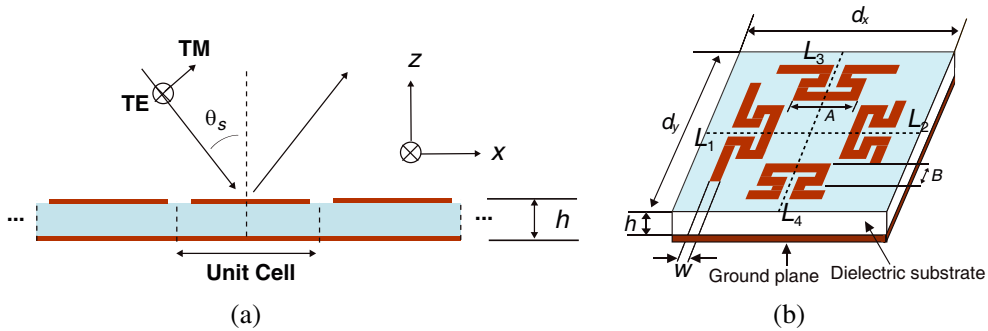
Figure 3. Analysis parameters for MoM. (a) Definition of coordinate system. (b) Structure of proposed element.

dielectric loss and the conductor loss are not included in the reflection phase analysis because of the losses are less than about 0.1 dB. A unit cell is divided into sub-cells (32×32) in the MoM analysis, and also the number of Floquet modes is 192 in the x and y directions.

3.2. Combination of the Element's Lengths

To realize broadband property, reflecting elements are required to provide the linear phase slope for the frequency. So, we have investigated the phase property for various element lengths $L_1(= L_3)$ and $L_2(= L_4)$. Figs. 4(a) and (b) shows the reflection phase response for the TE and the TM incidences on various combinations between lengths of L_2 and L_4. We can see from this figure that the phases for both the incidences have almost linear property for combination of the element's lengths $L_1(= L_3) = 11.4$ [mm] and $L_2(= L_4) = 8.4$ [mm]. Hereafter, we fix difference of the length $L_1(= L_3) - L_2(= L_4)$ to be 3.0 mm without depending on the length $L_1(= L_3)$.

3.3. Characteristics of Proposed Elements

Figure 5 shows the geometries for constructing a reflectarray antenna. Their reflection phase properties for the TE and the TM incidences are shown in Figs. 6(a) and (b), respectively. It is clear from this figure that the phases have the linear properties with almost the same slope, and also provide phase-shift range 360° over the wide frequency range. Fig. 7 shows the reflection phase properties of the element #1 and #12 for the different incident angles of the TE and the TM incidences. The phase curves are almost the same for the incident angle less than 50°. Figs. 8(a) and (b) shows the amplitude properties of cross polarization for both the incidences, and also Fig. 9 shows comparison of the average of the cross-polarization level for two types of the element. We can see that the average cross-polarization level of the proposed elements is lower than previous one from 14 GHz to 18 GHz.
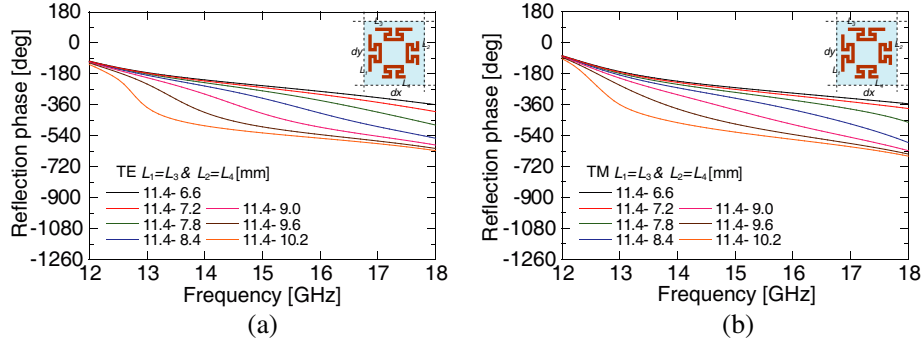
Figure 4. Combination of the element's lengths between $L_1(= L_3)$ and $L_2(= L_4)$. (a) TE incidence. (b) TM incidence.
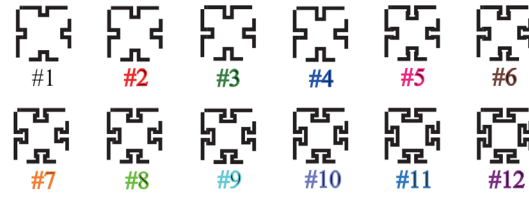
Figure 5. Geometries for the reflectarray design.
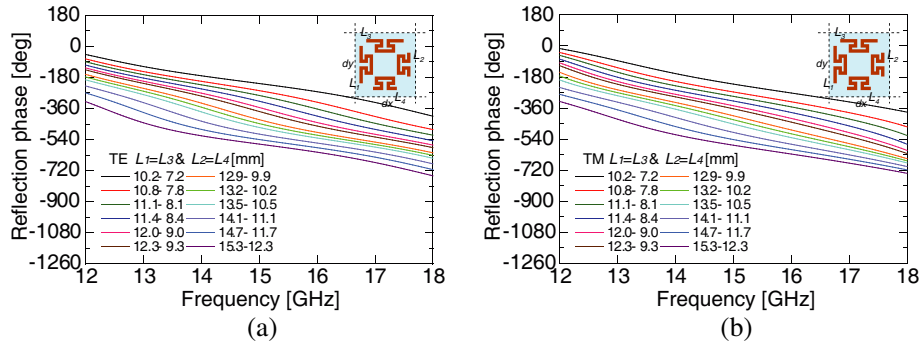
Figure 6. Frequency responses of the reflection phase for the TE and the TM incidences. (a) TE incidence. (b) TM incidence.
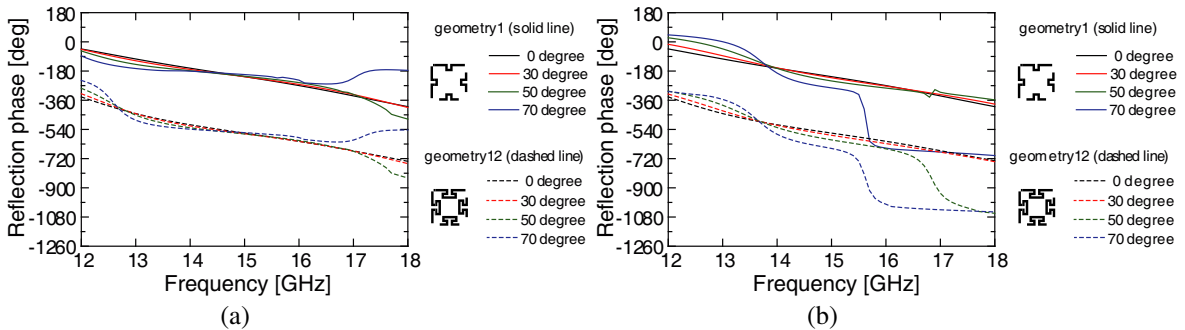
Figure 7. Reflection phase properties for the difference incident angle. (a) TE incidence. (b) TM incidence.
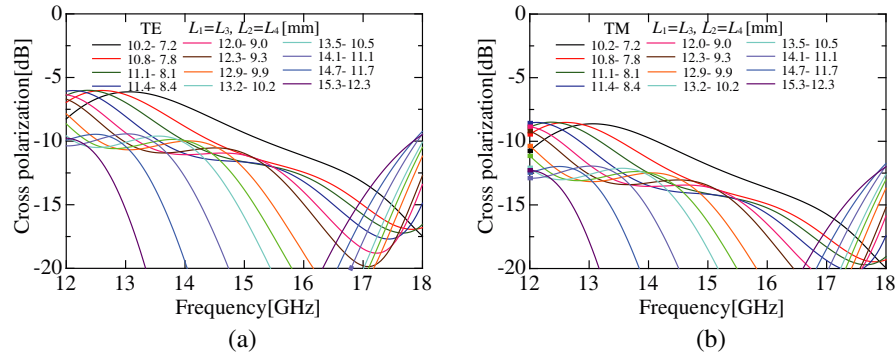
Figure 8. Cross-polarization level for the TE and the TM incidences. (a) TE incidence. (b) TM incidence.
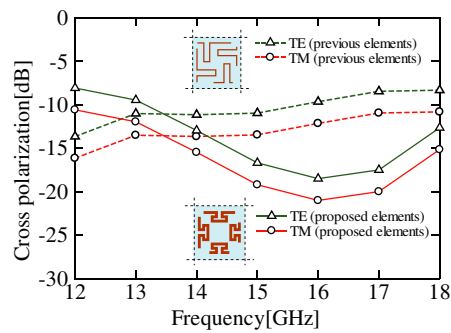
Figure 9. Comparison of the average of cross-polarization level for the TE and the TM incidences.

4. REFLECTARRAY DESIGN

4.1. Design Example

We now design an offset feed reflectarray with square aperture of dimension 153.6 mm × 153.6 mm (256 cells) constructed by the proposed elements (#1–#12) at the Ku-band. The arrangement of the reflectarray antenna is shown in Fig. 10. The degradation of its gain keeps less than 0.35 dB in the
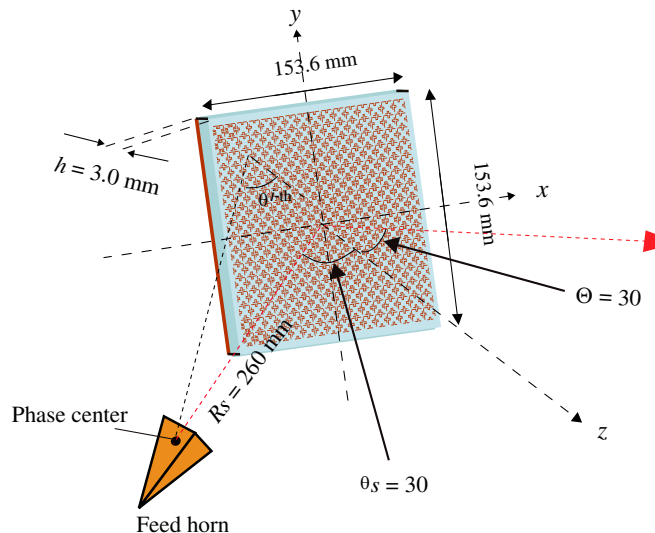
Figure 10. Design example of a reflectarray antenna.

case of the reflectarray elements having the phase of 30° interval [18]. In linear array design, it is often treated as an optimization problem of the minimizing number of elements by using compressive-sensing algorithm [19]. However, we didn't deal with the problem of minimizing the number of elements by the sparse array layout because our analysis is based on the periodic array. An offset angle of a primary illuminater is $\theta_s = 30°$ and the reflected angle $\Theta = 30°$ (x-z plane). The distance between its phase center and the center of the reflectarray is chosen to be 260 mm and the edge level on the reflectarray is -15 dB. For the offset feed at $\theta_s = 30°$, the angle incident to the element takes the range from 7° to 47°. As a result, we design all elements to have the desired phase properties corresponding to the incident angle.

5. NUMERICAL AND EXPERIMENTAL EVALUATION

Figures 11(a) and (b) show the top view of the designed reflectarray antenna and the fabricated reflectarraay antenna, respectively. The copper strips with thickness 18 μm are photo-etched on a thin dielectric film (Polyimide) with thickness 125 μm and the interval between the film and the ground plane is kept constant by a polyfoam (dielectric constant $\epsilon_r = 1.68$) with thickness $h = 3.0$ [mm]. Fig. 12 shows comparison of the radiation patterns between the calculated and the measured results for the TE and the TM incident waves at 14 GHz, 15 GHz and 18 GHz. The calculated far-field patterns are obtained by using the aperture field method [20]. It is clear from these figures that the main-beam patterns for both the incident waves agree well with each other. Moreover, the measured cross-polarization level for the main-beam is almost suppressed less than about -15 dB. Figs. 13 and 14 show comparison of the gain and the aperture efficiency between the calculated and the measured values, respectively. The calculated and the measured gains at the center frequency 15 GHz are 26.1 dB and 25.8 dB for the TE incidence, and 26.1 dB and 25.3 dB for the TM incidence, respectively. And aperture efficiencies are 54.7% and 51.4% for the TE incidence, and 54.7% and 46.1% for the TM incidence, respectively. Fig. 15 shows comparison of the measured cross-polarization level normalized by peak gain between the previously proposed elements [14] and the proposed ones. We can see that the previous shape generates the un-negligible cross-polarization component more than -10 dB because the height of the element's convex is too high, while the proposed elements have low cross-polarization property over the wide frequency range. These results verify that the Omega-shaped elements presented here are useful for wideband use with both dual-polarization and low cross-polarization properties.
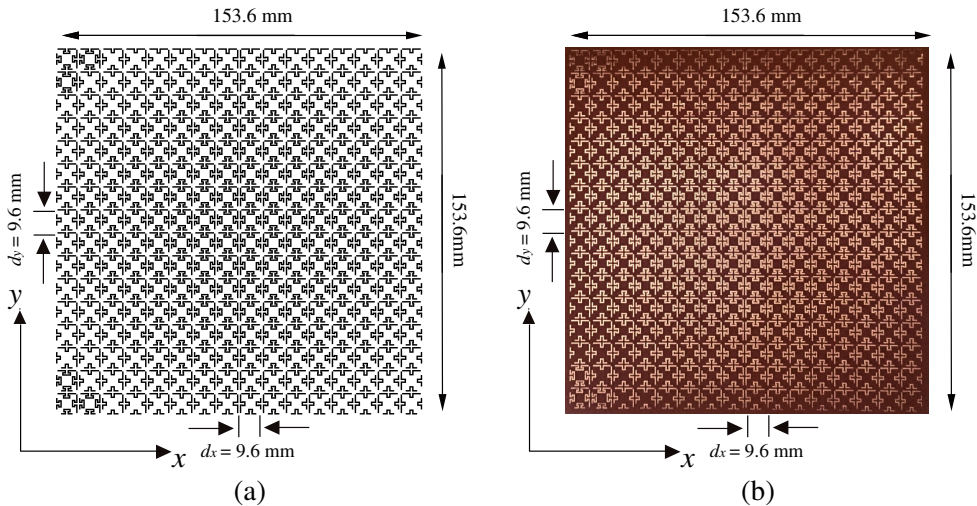
Figure 11. Designed and fabricated reflectarray antenna. (a) Designed reflectarray. (b) Fabricated reflectarray antenna.
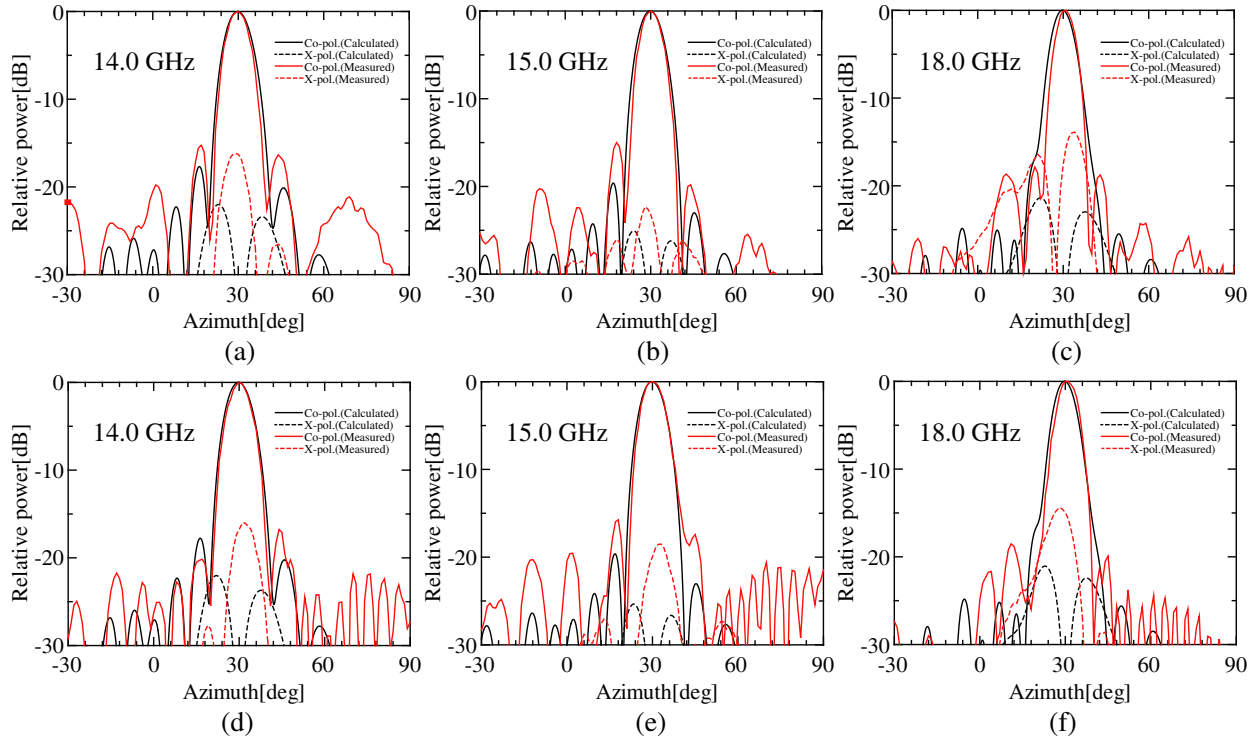
Figure 12. Radiation patterns for the TE and the TM incidences. (a) TE (14 GHz). (b) TE (15 GHz). (c) TE (18 GHz). (d) TM (14 GHz). (e) TM (15 GHz). (f) TM (18 GHz).
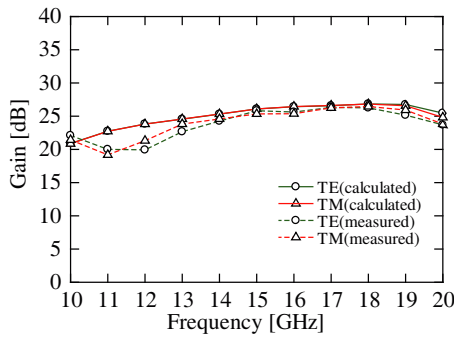
Figure 13. Comparison of gains between the calculated and the measured values.
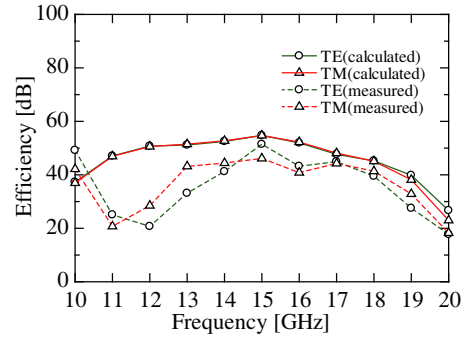
Figure 14. Comparison of aperture efficiency between the calculated and the measured values.
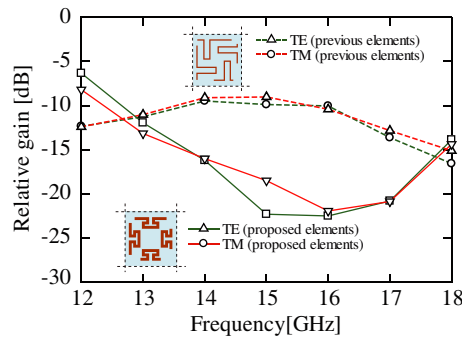
Figure 15. Comparison of measured cross-polarization level normalized by peak gain between the previous elements and proposed ones.

6. CONCLUSION

A reflectarray with the low cross-polarization as well as dual-polarization use for wideband has been presented by using the Omega-shaped element. The reflection phase characteristics for a set of the proposed elements have linear properties and almost the same curve-slope for the TE and the TM incidences. Moreover, the phase-shift range at the fixed frequency for the proposed set of the elements is more than 360° for both incidences. The average cross-polarization level of the proposed elements is lower than previous one from 14 GHz to 18 GHz. The reflectarray with the proposed elements has been designed and fabricated. The measured main-beam patterns agree well with the calculated values for both incidences. The calculated and measured values of the gain at the center frequency 15 GHz are 26.1 dB and 25.8 dB for the TE incidence, and 26.1 dB and 25.3 dB for the TM incidence, respectively. The aperture efficiencies are 54.7% and 51.4% for the TE incidence, and 54.7% and 46.1% for the TM incidence. The cross-polarized field is suppressed less than about −15 dB from 14 GHz to 18 GHz.

ACKNOWLEDGMENT

REFERENCES

1. Huang, J. and J. A. Encinar, *Reflectarray antennas*, Wiley, New Jersey, 2007.
2. Huang, J., V. Feria, and H. Fang, "Improvement of the three-meter Ka-band inflatable reflectarray antenna," *IEEE Int. Symp. Antennas Propagat.*, Vol. 1, 122–125, Jul. 2001.
3. Dietlein, C., A. Hedden, and D. Wikner, "Digital reflectarray considerations for terrestrial millimeter-wave imaging," *Antennas and Wireless Propagation Letters, IEEE*, Vol. 11, 272–275, Mar. 2012.
4. Li, L., Q. Chen, Q. Yuan, K. Sawaya, T. Maruyama, T. Furuno, and S. Uebayashi, "Frequency selective reflectarray using crossed-dipole elements with square loops for wireless communication applications," *IEEE Trans. Antennas Propag.*, Vol. 59, No. 1. 89–98, Jan. 2011.
5. David, F., M. Pozar, S. D. Targonski, and H. D. Syrigos, "Design of millimeter wave microstrip reflectarrays," *IEEE Trans. Antennas Propag.*, Vol. 45, No. 2, 287–296, Feb. 1997.
6. Qin, P., Y. J. Guo, and A. R. Weily, "Broadband reflectarray antenna using subwavelength elements based on double square meander-line rings," *IEEE Trans. Antennas Propag.*, Vol. 64, No. 1, 378–383, Jan. 2016.
7. Encinar, J., "Design of two-layer printed reflectarrays using patches of variable size," *IEEE Trans. Antennas Propag.*, Vol. 49, No. 10, 1403–1410, Oct. 2001.
8. Florencio, R., J. Encinar, R. Boix, and G. Perez-Palomino, "Dual-polarisation reflectarray made of cells with two orthogonal sets of parallel dipoles for bandwidth and cross-polarisation improvement," *IET Microw. Antennas Propag.*, Vol. 8, 1389–1397, Jun. 2014.
9. Han, C., Y. Zhang, and Q. Yang, "A broadband reflectarray antenna using triple gapped rings with attached phase-delay lines," *IEEE Trans. Antennas Propag.*, Vol. 65, No. 5, 2713–2717, May 2017.
10. Deguchi, H., T. Idogawa, M. Tsuji, and H. Shigesawa, "Offset reflectarrays with dense microstrips for wideband use," *Proc. of ISAP 2005*, Vol. 1, 229–232, Aug. 2005.
11. Sakita, S., H. Deguchi, and M. Tsuji, "Single-layer microstrip reflectarray based on dual-resonance behavior," *Proceedings of International Symposium on Antennas and Propagation*, 1290–1293, 2007.
12. Mayumi, K., H. Deguchi, and M. Tsuji, "Wideband single-layer microstrip reflectarray based on multiple-resonance behavior," *IEEE Antennas Propagat. Symp. Digest*, No. s432p4, 2008.
13. Toyoda, T., H. Deguchi, M. Tsuji, and T. Nishimura, "Reflectarray elements based on two-resonance behavior for dual-polarization use," *Proceedings of International Symposium on Antennas and Propagation*, [FrP2-15] A09_1003, 2011.

14. Toyoda, T., D. Higashi, H. Deguchi, and M. Tsuji, "Broadband reflectarray with convex strip elements for dual-polarization use," *Proceedings of International Symposium on Electromagnetic Theory*, 2013.

15. Higashi, D., H. Deguchi, and M. Tsuji, "Omega-shaped resonant elements for dual-polarization and wideband reflectarray," *IEEE Antennas Propagat. Symp. Digest*, 809–810, 2014.

16. Wu, T. K., *Frequency Selective Surface and Grid Array*, Wiley, New York, 1995.

17. Mittra, R., C. H. Chan, and T. Cwik, "Techniques for analyzing frequency selective surfaces — A review," *Proc. IEEE*, Vol. 76, No. 12, 1593–1615, Dec. 1988.

18. Asada, T., H. Deguchi, and M. Tsuji, "Optimization of arbitrarily shaped elements suppressing cross-polarization component in reflectarray," *IEICE Technical Report*, EMT-13-148, Nov. 2013.

19. Morabito, A. F., A. R. Lagana, G. Sorbell, and T. Isernia, "Mask-constrained power synthesis of maximally sparse linear arrays through a compressive-sensing-driven strategy," *Journal of Electromagnetic Waves and Applications*, Vol. 29, No. 10, 1384–1396, 2015.

20. Silver, S., "Microwave antenna theory and design," *IET*, 1949.